

Group-III vacancy induced $\text{In}_x\text{Ga}_{1-x}\text{As}$ quantum dot interdiffusion

H. S. Djie,¹ O. Gunawan,² D.-N. Wang,¹ B. S. Ooi,^{1,*} and J. C. M. Hwang¹

¹*Center for Optical Technologies, Department of Electrical and Computer Engineering, Lehigh University, Bethlehem, Pennsylvania 18015, USA*

²*Department of Electrical Engineering, Princeton University, Princeton, New Jersey 08544, USA*

(Received 27 October 2005; revised manuscript received 17 January 2006; published 21 April 2006)

The impact of group-III vacancy diffusion, generated during dielectric cap induced intermixing, on the energy state transition and the inhomogeneity reduction in the InGaAs/GaAs quantum-dot structure is investigated. We use a three-dimensional quantum-dot diffusion model and photoluminescence data to determine the thermal and the interdiffusion properties of the quantum dot. The band gap energy variation related to the dot uniformity is found to be dominantly affected by the height fluctuation. A group-III vacancies migration energy H_m for InGaAs quantum dots of 1.7 eV was deduced. This result is similar to the value obtained from the bulk and GaAs/AlGaAs quantum-well materials confirming the role of SiO_2 capping enhanced group-III vacancy induced interdiffusion in the InGaAs quantum dots.

DOI: 10.1103/PhysRevB.73.155324

PACS number(s): 61.72.Ji, 78.55.Cr, 81.07.St, 52.40.Hf

I. INTRODUCTION

Over the last decade, the effect of electronic structure and optical property modification after atomic interdiffusion of semiconductor quantum-dot (QD) has been subjected to intense research.¹⁻³ Atomic migration and defect diffusions become prominent due to large surface to volume ratio in three-dimensional (3D) QD islands. Significant modification of shape, composition, strain distribution, size, and hence quantum properties of QDs have been observed after a modestly high temperature treatment.⁴⁻⁹ The interdiffusion can be either strongly minimized or, on the contrary, be employed intentionally to improve the crystal quality and to tune the QD properties for various novel optoelectronic QD device applications. In any case, an in-depth understanding of the diffusion mechanism is fundamentally important for many aspects of semiconductor nanostructures.

In contrast to the well-established interdiffusion in quantum well (QW) structures, a comprehensive study of QD interdiffusion remains sparse and difficult. The well-established material characterization techniques for QW interdiffusion study such as Auger electron spectroscopy,¹⁰ secondary ion mass spectroscopy,¹¹ and Rutherford backscattering spectrometry¹² are not suitable for the analysis of interdiffusion in QD systems, primarily due to sputter erosion and detection resolution limit of these techniques. Although the cross-sectional tunneling and transmission electron microscopy gives an atomic-scale resolution to probe the atomic interdiffusion,¹³ this destructive technique is complex and requires the measurement of large number of samples to complete a meaningful experiment. This leads to a large accumulative error for the highly inhomogeneous self-assembled QDs.

A combination of theoretical diffusion model for a given interdiffused band profile and a nondestructive photoluminescence (PL) measurement has been applied to study the kinetic interdiffusion process in QW with high sensitivity especially at the early stage of interdiffusion.^{14,15} This simple approach relies on an accurate interdiffusion model to precisely quantify the interdiffusion process by calculating the

energy transition from the energy shift obtained from the experiment. However, this analysis technique has not been successfully transferred to the study of QD systems primarily due to the lack of a reliable theoretical model for 3D interdiffusion calculation.¹⁶⁻²⁰

In this study, we perform both experimental and theoretical studies to investigate the effect of annealing induced interdiffusion in InGaAs/GaAs QD material. To probe the role of surface diffusion, the extent of interdiffusion in QD is locally suppressed or enhanced by the dielectric cap encapsulant layers, which subsequently control the surface vacancy generated during high temperature annealing and promote the vacancy-mediated diffusion.^{21,22} The experimental results from photoluminescence (PL) and transmission electron microscopy (TEM) were correlated with the theoretical calculation to determine the effect of interdiffusion on the electronic energy levels and energy variation in the dot assembly. The diffusion coefficient and activation energy related to the vacancy migration were determined and compared to those reported results to assess the diffusion mechanism in QD material.

II. EXPERIMENTS

The $\text{In}_{0.6}\text{Ga}_{0.4}\text{As}$ QDs were grown by molecular beam epitaxy technique on Si-doped (100)-oriented GaAs substrates. A 1500-nm-thick $\text{Al}_{0.3}\text{Ga}_{0.7}\text{As}$ lower cladding layer was first grown, which was followed by a superlattice of 20 pairs of 2 nm $\text{Al}_{0.3}\text{Ga}_{0.7}\text{As}$ and 2 nm GaAs. Five InGaAs dot layers were then consecutively grown, with each dot layer comprising five pairs of alternating InAs and GaAs submonolayers. Under a constant arsenic flux, growth was interrupted after each monolayer in order to stabilize the surface. GaAs spacers 40 nm thick were inserted between the QD layers. The dots formation was established and monitored by reflection high-energy electron diffraction. The bulk and superlattice layers were all grown at typical substrate temperatures of $\sim 600^\circ\text{C}$, while the QD layers were grown at $\sim 515^\circ\text{C}$.

QD samples were capped with 200-nm thick SiO_2 and Si_xN_y caps deposited using plasma enhanced chemical vapor deposition. The refractive index of the deposited SiO_2 and Si_xN_y layers, measured using ellipsometry at the wavelength of 633 nm, are 1.42 and 2.35, respectively. The data indicate that a stoichiometric SiO_2 film is well formed while the Si_xN_y film is a Si-rich film. The samples were repetitively annealed in nitrogen ambient for up to four cycles, with 2 min per cycle, at temperatures from 650 to 850 °C using a rapid thermal processor. References were obtained from bare samples annealed under similar process conditions. Two fresh pieces of GaAs proximity caps were used to provide As over pressure during the annealing. TEM images were taken from the (002) dark field along the [011] zone axis to analyze the chemical composition of the quantum dots. PL spectra were measured 77 K using 532 nm diode pumped solid state laser as the excitation source. In the setup, the low excitation power of less than 100 W/cm² was determined to excite only the ground state transition (E_{e0-hh0}).

III. THEORETICAL MODEL

We have developed a 3D quantum nanostructure model, as detailed elsewhere,²³ to calculate the electronics states of the interdiffused QDs. This model solves the Hamiltonian using BenDaniel-Duke equation in momentum space. Assuming an isotropic interdiffusion process as first order approximation, the interdiffusion of the indium concentration (x) at any point in space should obey Fick's law of diffusion. In reciprocal space, it yields a simple solution

$$x_{\mathbf{K}}(L_d) = x_{\mathbf{K}}^{-k^2 L_d^2}, \quad (1)$$

which means that the interdiffusion effect attenuates the Fourier components ($x_{\mathbf{K}}$) by a factor of $e^{-k^2 L_d^2}$ where \mathbf{K} is the reciprocal lattice vector that runs through all lattice points in the reciprocal space, L_d is the diffusion length representing the degree of interdiffusion given by $L_d = \sqrt{D_x t_a}$ where D_x is the group-III diffusion coefficient, t_a is the diffusion time associated with annealing time. From Eq. (1), any $\text{In}_x\text{Ga}_{1-x}\text{As}$ QD parameters that vary linearly with the indium concentration x will have similar solution. The biaxial in-plane strains perpendicular to growth direction z and the uniaxial shear strain parallel to z also vary according to the alloy composition after interdiffusion.²⁴ The change in dot composition profile after interdiffusion modifies the confinement profile, hence the ground state energy transition, E_{e0-hh0} . The shift in ground state energy, $\Delta E_{e0-hh0} = E_{e0-hh0}^{L_d=0} - E_{e0-hh0}^{L_d>0}$, after diffusion length L_d depends on the value of D_x , which is a function of temperature. The parameters for the as-grown QD used in the calculation are based on a lens-shaped $\text{In}_{0.6}\text{Ga}_{0.4}\text{As}$ QD configuration from the cross-sectional TEM image of as-grown QDs as shown in Fig. 1(a).

IV. RESULTS AND DISCUSSION

Figure 1(a) depicts the composition-sensitive (002) dark-field TEM images from the as-grown QDs. The dislocation-

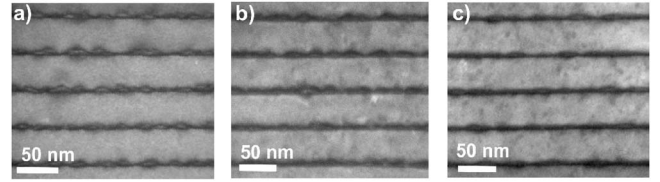


FIG. 1. Cross-sectional (002) dark-field TEM images along the [011] zone axis from the InGaAs QD structures: (a) as grown and after annealing at (b) 700 °C and (c) 800 °C for 2 min.

free InGaAs dots embedded in the surrounding GaAs matrix as revealed from the contrast in (002) dark-field image. The average lens-shaped QDs have a height of 4.8 ± 0.5 nm, a diameter of 28 ± 8 nm, and an inter-dot spacing of ~ 5 nm. The size dispersion is estimated to be 10% from the cross-sectional TEM analysis. The calculated ground state energy transition, E_{e0-hh0} , of 1.12 eV is consistent with the measured PL peak at 77 K from the as-grown QDs (Fig. 2). The broad linewidth of 63 meV is attributed to the simultaneous excitation from laser beam to $\sim 10^6$ dots, which consists of a relatively large dot assembly with size and compositional fluctuation. The size dispersion leads to the variation in the luminescence energy. Our observation corroborates an earlier report that the typical inhomogeneity of dot size at $\pm 10\%$ gives PL linewidth of 60–80 meV.²⁵ The mismatch from dots and GaAs barrier produces a strain/displacement field around dots leading to the TEM image contrast of (004) bright field. It reveals the compressive and tensile strain accumulation above and below each dot, respectively.

The high temperature annealing process significantly affects the band gap energy by smearing the interfaces between QDs and GaAs barriers resulting from the interdiffusion of In-Ga atoms. Figure 1(b) and 1(c) show TEM images revealing the structural transformation after annealing at 700 and

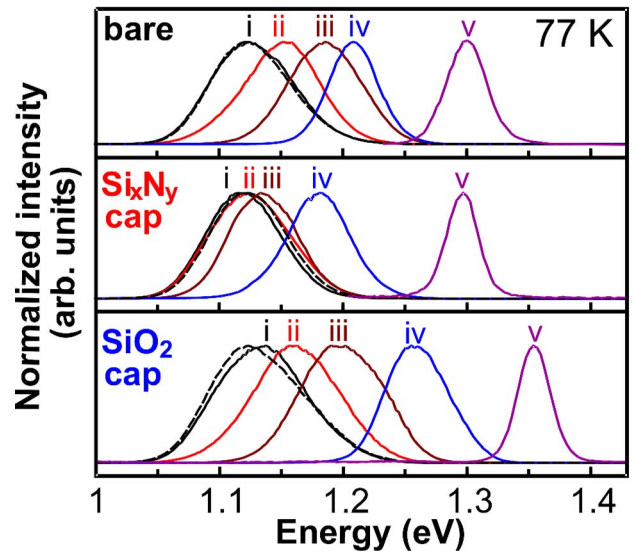


FIG. 2. (Color online) The PL spectra at 77 K from the bare, Si_xN_y capped, and SiO_2 capped QDs after annealing at (i) 650, (ii) 700, (iii) 750, (iv) 800, and (v) 850 °C. The spectrum of as grown is included (dotted line).

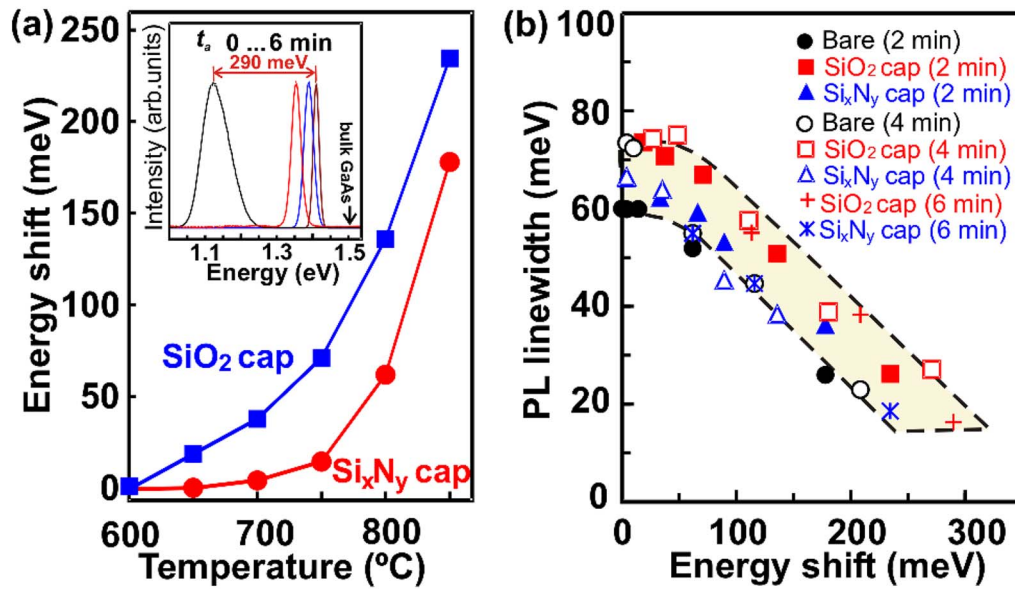


FIG. 3. (Color online) (a) The band gap shift summary after annealing for 2 min for SiO_2 (square) and Si_xN_y (circle) capped QDs. The inset is PL spectra from SiO_2 capped QDs annealed repetitively at 850°C . (b) The PL linewidth vs the band gap shift at different annealing caps and durations. The shaded area within dashed line is a guide for eye only.

800°C , respectively. In Fig. 1(b), QDs remain well separated with improvement in the height uniformity after annealing at 700°C . The intermixing degree is further enhanced as the temperature increases from 700 to 800°C . The dot height becomes more uniform as annealing proceeds to beyond the measurement limit of our TEM system. The QDs assume a flat top and are merged into a continuous layer of quasi well as shown in Fig. 1(c) after annealing at 800°C . No dislocation was observed from all annealed structures even after the dots coalesce into quasi wells.

The structural transformation of dot subjected to interdiffusion alters the potential confinement, and hence the energy transition of the annealed dots. Figure 2 depicts the PL spectra from the bare (uncapped), SiO_2 capped, and Si_xN_y capped QDs annealed at various temperatures for 2 min. The energy blueshift was found to increase with increasing annealing temperature for all samples. Si_xN_y capped QD samples exhibit a lower degree of band gap shifts than SiO_2 capped samples as summarized in Fig. 3(a). The shift in Si_xN_y capped QDs is attributed to the intrinsic defects induced self-diffusion in QDs.^{21,22} A slight increase in the intermixing degree is observed from the bare sample annealed under similar conditions. In addition to the intrinsic defect induced intermixing, the small degree of intermixing observed here might be ascribed to the arsenic loss in the bare sample even they were annealed with GaAs proximity caps. An energy shift as small as 14 meV has been measured from the Si_xN_y capped QDs after annealing up to 750°C . Under similar annealing condition, a band gap shift of about 70 meV has been observed from the SiO_2 capped QDs. At 850°C and above, the differential energy shift between the SiO_2 and Si_xN_y capped QDs reduces, suggesting that thermal induced interdiffusion effect dominates under this annealing condition. Systematical reduction of PL linewidth has been observed from all samples. The inset of Fig. 3(a) presents PL

spectra evolution for SiO_2 capped QDs after repetitive annealing at 850°C for up to three cycles, for 2 min each cycle. The arrow represents the 77 K PL peak position of the bulk GaAs material. A blueshift as large as 290 meV has been observed from QDs annealed for three repetitive cycles, with the corresponding spectrum linewidth of ~ 16 meV. The linewidth observed is a factor of 4 narrower than the as-grown QDs indicating a significant improvement in dot size dispersion for the annealed QDs. Figure 3(b) summarizes the PL linewidth dependence to the QD energy blueshift. The linewidth stays constant for the samples with blueshift up to 50 meV, and drops almost linearly for samples intermixed to more than 50 meV band gap shift.

Inhomogeneity of QDs is an intrinsic property of the self-assembled QDs. This undesirable property contributes to the finite linewidth broadening of the luminescence spectra. Considering many factors that determine the electronics states of the QDs, it is essential to identify the dominant parameters that affect the transition state of the interdiffused QDs. Using our model, we investigate the inhomogeneity of QDs by evaluating the sensitivity of the various QD geometrical parameters to the energy states at different degrees of interdiffusion. These parameters are dot height (h), base width (b), inter-dot lateral spacing (a), volume (V_{QD}) and In composition (x). Figure 4(a) summarizes the energy variation, $\Delta E_{e0-hh0}^{\pm 10\%}$, as a result of 10% variation in corresponding QD parameters,^{25,26} versus the energy shift ΔE_{e0-hh0} that corresponds to the degree of interdiffusion. In the case of the as-grown QD ($\Delta E_{e0-hh0}=0$), in composition and height variation are the most sensitive parameters that determine the QDs energy variation. This result qualitatively provides an explanation to inhomogeneity reduction techniques related to the control of height and compositional dispersion in self-formed QD assembly.²⁸⁻³⁰ As the interdiffusion proceeds, the fluctuation of In composition results in a linear decrease in

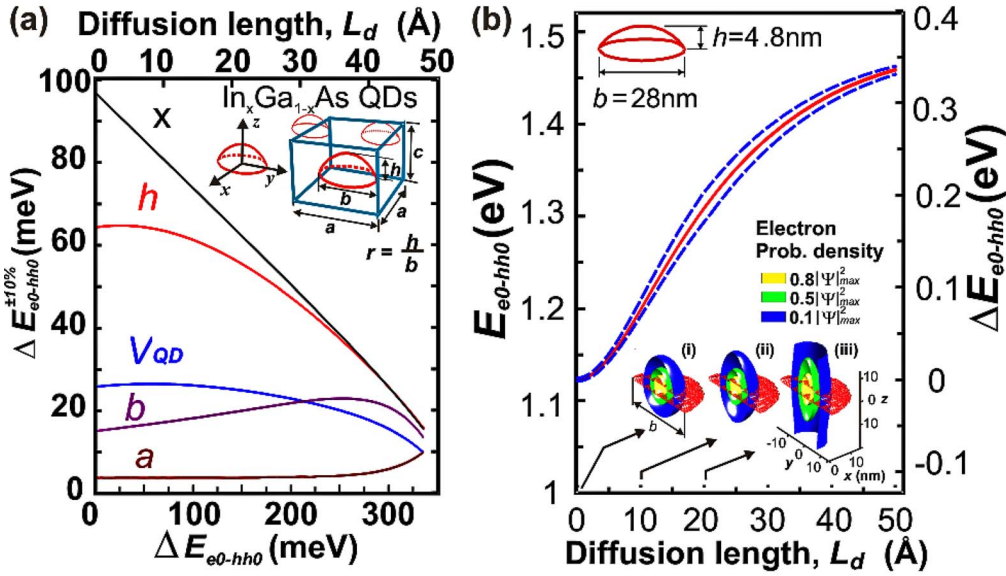


FIG. 4. (Color online) (a) The band gap shift variation against the energy blueshift from reference lens-shaped InGaAs QDs ($b=28$ nm, $h=4.8$ nm, $a=33$ nm, $c=40$ nm) with the 10% fluctuation in the QD parameters. For volume variation, the aspect ratio h/b is kept constant. (b) The calculated QD ground state transition energy against diffusion length. The inset shows half cross section of ground state electron probability density and the confinement potential at L_d of (i) 0 Å, (ii) 10 Å, and (iii) 20 Å.

energy variation. In the case of the height fluctuation, however, the energy variation stays constant initially, and gradually decreases as interdiffusion proceeds. This height variation effect is consistent with our experimental data of PL linewidth evolution in Fig. 3(b), where initially the luminescence linewidths (i.e., $\Delta E_{e0-hh0} < 50$ meV) stay constant and then drop as the interdiffusion proceeds. The TEM images showing QDs with improved height uniformity after annealing is consistent with the inhomogeneity reduction of ground state transition energies as observed from the PL spectra.

The fact that height h is the most sensitive parameter affecting the QD energy states is not surprising since, in our samples, the QD height is the smallest and therefore the most critical dimension that determines the confinement potential. Our observation is also well supported by previous studies.^{9,26} This result implies a possible reduction in dot inhomogeneity using interdiffusion process especially in the closely stacked QDs, where the wave functions of the individual QD layers are strongly coupled and the height uniformity is difficult to control during the epitaxial growth.

Interdiffusion of In and Ga atoms at the dot-barrier interface causes an increase of the ground state transition energy as plotted in Fig. 4(b). The dashed line depicts an estimated theoretical uncertainty from our interdiffusion model. The uncertainty reflects the reduced error at lower L_d due to the fact that for zero blueshift, the diffusion length is 0 Å. At large L_d the carriers in the QD become less confined as indicated by a larger spread of the wavefunction. At similar L_d thicker dot (higher h) gives a larger degree of band gap shift than the thin dot (lower h) causing a decrease in the energy sensitivity $\Delta E_{e0-hh0}^{\pm 10\%}$. A significant interdiffusion occurs in the early stage of L_d . Beyond this, the interdiffusion rate becomes less pronounced. The saturation phenomenon in energy shift occurs at $L_d > 50$ Å at which the transition energy

approaches the band gap energy of the GaAs bulk material indicating a complete dissolution of dot to the surrounding GaAs barrier,²⁷ that suggests a maximum band gap tunability of 370 meV. However, before we reach this limit, at $L_d \sim 40$ Å the QD confinement becomes too weak so that we fail to observe any PL signal beyond this diffusion length.

The experimental data of the annealed bare QDs were analyzed using our numerical model that relates the energy blue-shifts to the diffusion length. Figure 5(a) presents the square dependence of diffusion length L_d^2 to the annealing time t_a . Reasonably good linear fit to the data, where the slope yield the diffusion constant D_x , is obtained. It follows

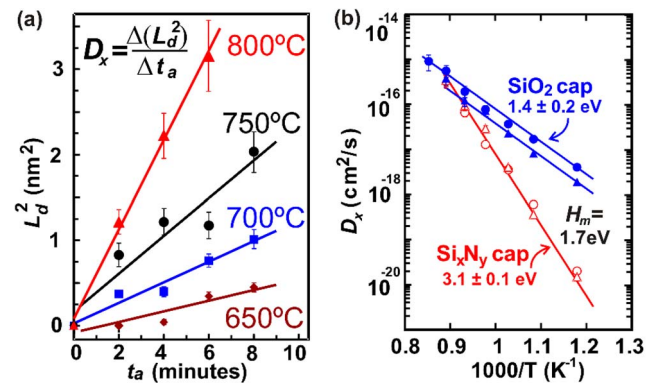


FIG. 5. (Color online) (a) Square dependence of L_d , as a function of annealing duration from 2 to 8 min from the bare QDs. The solid lines represent the theoretical fit from the experimental data to determine D_x . (b) The Arrhenius plot of diffusion coefficient at annealing temperature between 550 and 900 °C for 2 min deduced from 20-stack QDs embedded in 40 nm (50 nm) thick GaAs matrix shown as circle (triangle) data points. Samples with SiO₂ (Si₃N₄) cap are shown as solid (hollow) data points.

the Fickian diffusion process, which is independent of In composition in QDs. Diffusion constants D_x determined from the slope of a least-square fit are $1.0 \times 10^{-17} \text{ cm}^2/\text{s}$ at 650°C , $2.0 \times 10^{-17} \text{ cm}^2/\text{s}$ at 700°C , $3.7 \times 10^{-17} \text{ cm}^2/\text{s}$ at 750°C , and $8.7 \times 10^{-17} \text{ cm}^2/\text{s}$ at 800°C . D_x increases monotonically as the temperature increases.

The activation energy corresponds to the energy associated with the motion and formation of defects in the interdiffusion process. The temperature dependence of the diffusivity can be described by Arrhenius equation $D_x \sim \exp(-E_A/kT)$, where T and E_A refer to the annealing temperature and the activation energy, respectively. In the case of equilibrium linear diffusion, the activation energy is the sum of the V_{III} formation energy and the V_{III} migration energy ($E_A = H_f + H_m$) in group-III atoms. The experimental data D_x is linearly fitted over $1000/T$, as shown in Fig. 5(b). For completeness, the experimental data from 20-stack QDs embedded in 50-nm-thick GaAs matrix grown under similar growth conditions were also included.

It has been determined that thin film porosity and stress are two dominant effects in dielectric cap induced intermixing.³¹ E_A calculated from the slope of D_x is $3.1 \pm 0.1 \text{ eV}$ for both 5-stack and 20-stack Si_xN_y capped QDs annealed between 550 and 900°C . This value is in excellent agreement with early annealing studies on Si_xN_y capped QWs.^{32,33} This observation indicates that V_{Ga} generated in the Si_xN_y capped QD sample is minimum during annealing. The Si_xN_y layer used in our experiment was a dense Si-rich film with relatively high refractive index ($n=2.35$). As the film density is high, the out-diffusion of group-III and/or group-V elements from semiconductor to the Si_xN_y film is expected to be low during annealing. Further, the difference in the linear thermal expansion coefficient between the Si_xN_y layer ($\alpha=2.8 \times 10^{-6} \text{ }^\circ\text{C}^{-1}$) and GaAs-based material ($\alpha=6.8 \times 10^{-6} \text{ }^\circ\text{C}^{-1}$) is relatively small. This structure will induce small compressive strain in the QD sample that will further lock the out-diffusion of group-III elements into the thin film. The combination of all these effects contributes to small degree of the impurity-free vacancy induced diffusion in the QD structure. Hence, we conclude that the blueshift observed from the Si_xN_y cap samples is primarily due to the thermal shift associated with the intrinsic defects from the epilayers and QDs.

Compared to the Si_xN_y cap under similar range of annealing temperature, SiO_2 cap gives lower diffusion barriers and produces significantly low E_A at $1.4 \pm 0.2 \text{ eV}$. Compared to the thermally grown SiO_2 ($n=1.46$), SiO_2 used in our experiment has a slightly lower refractive index. This porous film acts as an effective sink for Ga out-diffusion. In addition, the thermal expansion coefficients of SiO_2 ($\alpha=0.52 \times 10^{-6} \text{ }^\circ\text{C}^{-1}$) are about ten times smaller than GaAs. The surface of QD sample is under a significant compressive stress during annealing. To release the stress,²² Ga atoms will preferentially out-diffuse into SiO_2 and promote atomic interdiffusion in the QD region. Here, we attribute the low E_A in SiO_2 capped QDs to the constant injection of Ga vacancies imposed by the strain field at the semiconductor

surface in the form of migration energy H_m for In-Ga interdiffusion. This characteristic serves to create a high V_{Ga} density near the surface to assist QD intermixing, and appears to play a fundamental role in enhance interdiffusion in QD using the dielectric cap annealing induced intermixing technique.

The energy of group-III vacancy in-diffusion comprises both vacancy migration energy H_m and vacancy formation energy H_f under Si_xN_y capped QDs, while it only contains vacancy formation energy H_f under SiO_2 capped QDs. The effective group-III surface vacancy migration energy H_m can be extracted from the difference between activation energy of Si_xN_y and SiO_2 capped QDs. A $H_m=1.7 \text{ eV}$ is deduced as a consequence of the surface vacancy enhanced QD interdiffusion in the SiO_2 capped QDs. The intermixed bare samples show an intermediate situation that is governed by the combination effect of the intrinsic interdiffusion and the surface out-diffusion due to the As loss even though the sample was annealed with GaAs proximity caps. H_m obtained from our analysis is consistent with the widely accepted value of $1.7\text{--}1.8 \text{ eV}$ for GaAs vacancy migration in the bulk and GaAs-based QW material.^{1,15,34,35} This result implies that neither the quantum structure nor the group-III atomic concentration significantly affect the vacancy migration behavior in the interdiffusion process. This also suggests the possibility of using unperturbed bulk values for vacancy migration analysis of more complex cases of 3D QD that involve multiple cations and/or anions interdiffusion.

The dot interdiffusion is enhanced in the SiO_2 capped QDs with respect to Si_xN_y capped QDs at low annealing temperature regime. At high temperature annealing $T > 800^\circ\text{C}$, the diffusion coefficients between SiO_2 and Si_xN_y capped QDs become comparable ($D_x \sim 10^{-16} \text{ cm}^2/\text{s}$) suggesting the less pronounced role of dielectric cap layers to induce interdiffusion at the high annealing temperature. Similar effect has been obtained from other QD systems.^{21,22,36} The result suggests that a large differential shift between SiO_2 and Si_xN_y capped QDs can only be obtained by processing the QD samples at $T < 800^\circ\text{C}$.

V. CONCLUSION

In summary, we have investigated the interdiffusion effect related to surface vacancy diffusion in the InGaAs/GaAs QDs at high temperature treatment. Annealing results in the reduction of luminescence linewidth and the blueshift in the ground state transition energy. From numerical analysis, we attribute the linewidth narrowing effect to the improvement of the quantum-dot height fluctuation. The interdiffusion behavior was assessed by correlating the photoluminescence results with the 3D theoretical model. The atomic interdiffusion in InGaAs/GaAs QDs follows the Fickian diffusion process, which is independent of In composition in QDs. We found a lower activation energy of $1.4 \pm 0.2 \text{ eV}$ in the SiO_2 cap than that of $3.1 \pm 0.1 \text{ eV}$ in the Si_xN_y cap. From these activation energies, a Ga vacancy migration energy H_m of 1.7 eV was obtained.

ACKNOWLEDGMENTS

The authors would like to thank Marvin H. White of the Sherman Fairchild Center for Solid State Studies, Lehigh University, for the support of the clean-room facility. This work is supported in part by the U.S. Army Research Labo-

ratory through Lehigh-Army Cooperation Agreement and the Pennsylvania Infrastructure Technology Alliance (PITA), a partnership of Carnegie Mellon University, Lehigh University and the Commonwealth of Pennsylvania Department of Community and Economic Development.

*Corresponding author. Electronic address: bsooi@lehigh.edu

- ¹J. L. Rouviere, Y. Kim, J. Cunningham, J. A. Rentschler, A. Bourret, and A. Ourmazd, *Phys. Rev. Lett.* **68**, 2798 (1992).
- ²W. P. Gillin and D. J. Dunstan, *Phys. Rev. B* **50**, 7495 (1994).
- ³J. H. Marsh, D. Bhattacharyya, A. S. Helmy, E. A. Avrutin, and A. C. Bryce, *Physica E (Amsterdam)* **8**, 154 (2000).
- ⁴I. Kegel, T. H. Metzger, A. Lorke, J. Peisl, J. Stangl, G. Bauer, J. M. Garcia, and P. M. Petroff, *Phys. Rev. Lett.* **85**, 1694 (2000).
- ⁵J. M. Garcia, G. Medeiros-Ribeiro, K. Schmidt, T. Ngo, J. L. Feng, A. Lorke, J. Kotthaus, and P. M. Petroff, *Appl. Phys. Lett.* **71**, 2014 (1997).
- ⁶I. Kegel, T. H. Metzger, A. Lorke, J. Peisl, J. Stangl, G. Bauer, J. M. Garcia, and P. M. Petroff, *Phys. Rev. Lett.* **85**, 1694 (2000).
- ⁷J. Tatebayashi, N. Hatori, M. Ishida, H. Ebe, M. Sugawara, Y. Arakawa, H. Sudo, and A. Kurumata, *Appl. Phys. Lett.* **86**, 053107 (2005).
- ⁸S. Malik, C. Roberts, R. Murray, and M. Pate, *Appl. Phys. Lett.* **71**, 1987 (1997).
- ⁹N. Perret, D. Morris, L. Franchomme-Fosse, R. Cote, S. Fafard, V. Aimez, and J. Beauvais, *Phys. Rev. B* **62**, 5092 (2000).
- ¹⁰L. L. Chang and A. Koma, *Appl. Phys. Lett.* **29**, 138 (1976).
- ¹¹S. A. Schwarz, T. Venkatesan, B. Bhat, M. Koza, H. W. Yoon, Y. Arakawa, and P. Mei, *Mater. Res. Soc. Symp. Proc.* **56**, 321 (1986); P. Mei, H. W. Yoon, T. Venkatesan, S. A. Schwarz, and J. P. Harbison, *Appl. Phys. Lett.* **52**, 1240 (1988).
- ¹²Z. H. Jafri and W. P. Gillin, *J. Appl. Phys.* **81**, 2179 (1997).
- ¹³R. S. Goldman, *J. Phys. D* **37**, R163 (2004).
- ¹⁴W. P. Gillin, D. J. Dunstan, K. P. Homewood, L. K. Howard, and B. J. Sealy, *J. Appl. Phys.* **73**, 3782 (1993).
- ¹⁵R. Geursen, I. Lahiri, M. Dinu, M. R. Melloch, and D. D. Nolte, *Phys. Rev. B* **60**, 10926 (1999).
- ¹⁶E. H. Li, B. L. Weiss, and K. S. Chan, *Phys. Rev. B* **46**, 15181 (1992).
- ¹⁷F. E. Prins, S. Y. Nikitin, G. Lehr, H. Schweizer, and G. W. Smith, *Phys. Rev. B* **49**, 8109 (1994).
- ¹⁸T. Stirner, *J. Chem. Phys.* **117**, 6715 (2002).
- ¹⁹S. Fafard and C. N. Allen, *Appl. Phys. Lett.* **75**, 2374 (1999).
- ²⁰J. A. Barker and E. P. O'Reilly, *Physica E (Amsterdam)* **4**, 231 (1999).
- ²¹D. Bhattacharyya, A. S. Helmy, A. C. Bryce, E. A. Avrutin, and J. H. Marsh, *J. Appl. Phys.* **88**, 4619 (2000).
- ²²L. Fu, P. Lever, H. H. Tan, and C. Jagadish, *Appl. Phys. Lett.* **82**, 2613 (2003).
- ²³O. Gunawan, H. S. Djie, and B. S. Ooi, *Phys. Rev. B* **71**, 205319 (2005).
- ²⁴S. L. Chuang, *Phys. Rev. B* **43**, 9649 (1991).
- ²⁵M. Grundmann and D. Bimberg, *Phys. Rev. B* **55**, 9740 (1997).
- ²⁶Y. Ebiko, S. Muto, D. Suzuki, S. Itoh, K. Shiramine, T. Haga, Y. Nakata, and N. Yokoyama, *Phys. Rev. Lett.* **80**, 2650 (1998).
- ²⁷A. Babinski, J. Jasinski, R. Bozek, A. Szepielow, and J. M. Baranowski, *Appl. Phys. Lett.* **79**, 2576 (2001).
- ²⁸E. C. Le Ru, P. Howe, T. S. Jones, and R. Murray, *Phys. Rev. B* **67**, 165303 (2003).
- ²⁹P. B. Joyce, T. J. Krzyzewski, G. R. Bell, T. S. Jones, E. C. Le Ru, and R. Murray, *Phys. Rev. B* **64**, 235317 (2001).
- ³⁰S. Fafard, Z. R. Wasilewski, C. N. Allen, D. Picard, M. Spanner, J. P. McCaffrey, and P. G. Piva, *Phys. Rev. B* **59**, 15368 (1999).
- ³¹P. N. K. Deenapanray and C. Jagadish, *Electrochem. Solid-State Lett.* **4**, G11 (2001).
- ³²S. S. Rao, W. P. Gillin, and K. P. Homewood, *Phys. Rev. B* **50**, 8071 (1994).
- ³³O. M. Khreis, W. P. Gillin, and K. P. Homewood, *Phys. Rev. B* **55**, 15813 (1997).
- ³⁴D. E. Bliss, W. Walukiewicz, J. W. Ager, E. E. Haller, K. T. Chan, and S. Tanigawa, *J. Appl. Phys.* **71**, 1699 (1992).
- ³⁵I. Lahiri, D. D. Nolte, M. R. Melloch, J. M. Woodall, and W. Walukiewicz, *Appl. Phys. Lett.* **69**, 239 (1996).
- ³⁶We also observed experimentally the similar IFVD enhancement for various quantum heterostructures, i.e., GaAs/AlGaAs QW, InGaAs/InGaAsP QW, InAs/InP QD, and InAs/InAlGaAs QD.